Field Test and Analysis of Everyday Train-induced Ground Motions

Contents

Summary

Study Design

We investigate the concern that the vibrations caused by small earthquakes, that are generally not felt, could, if frequent enough, result in damage to buildings in Groningen. We are thus particularly interested in understanding whether exposing buildings to frequent vibrations with velocities smaller than 3 $^{mm}/_{s}$ could result in damage.

For a single exposure to such a small earthquake there is widespread international consensus that these small earthquakes, categorized below the EMS intensity VI that is the lowest intensity level where building damage is expected to occur. At this level, the perception is described as: "*Many people are frightened and run outdoors.*" and "*Many houses suffer slight non-structural damage like hair-line cracks and fall of small pieces of plaster.*" Clearly the small earthquakes in Groningen do not fit in with EMS intensity VI and thus will cause no damage from such an earthquake.

We acknowledge however that the above-stated assessment does not address the impact of the repetitive occurrences of smaller earthquake vibrations on buildings. Laboratory experiments show no damage when structures are exposed to multiple events of vibrations below a velocity of 3 $^{mm}/_{s}$. However, this could be a result of laboratory conditions and the state of the buildings sampled in the experiments. Exposing the existing buildings to the levels of vibrations of interest in a controlled laboratory environment is currently not a viable option.

Road and rail transportation is a known and well understood cause of vibrations in the ranges discussed above and regularly exposes many buildings to those vibration levels [1, 3 and 4]. Because trains provide a more controlled vibration source, an array of geophones was placed near a railroad track to monitor ground motions continuously for a period of 56 days. By investigating the vibrations caused by trains, we attempt to contextualise the impact of small vibrations resulting from earthquakes on buildings. Here we can build on the year-long experience of ProRail [1]:

"It almost never happens that vibrations caused by trains are so strong that a building gets damaged. These vibrations – as opposed to an earthquake - are not strong enough to affect the construction of a building."

Focus of this study is not the impact of stronger vibrations near the epicentre of a larger earthquake, but the impact of (1) repeated vibrations caused by low magnitude earthquakes at short epicentral distances or (2) vibrations caused by higher magnitude earthquakes at larger epicentral distances, which are comparable in strength to vibrations caused by trains. Trains expose buildings to these vibrations on a weekly and sometimes even daily basis almost never causing damage [1]. In comparison, exposure rates resulting from earthquake vibrations in Groningen are much lower.

The results of this study are relevant for the discussion on building damage in the outer areas of Groningen (the so-called "buitengebied"), where earthquake vibrations have been limited but many damage claims have been made.

Conclusions

This report describes the peak ground velocity (PGV) measured along a section of the railroad track in Groningen province, the Netherlands, and provides an estimate of the exposed number of houses located near a track. Over the period of 56 days, PGV exceeded $1^{mm}/_{s}$ nearly 2,000 times along a ~100m geophone array situated 15m from the railroad track; not all the measured exceedances were caused by trains. Some were caused by other urban noise sources. This level of ground motion is comparable in duration and frequency content to measurements made as close as ~6.5km epicentral distance to the M3.4 Zeerijp earthquake of 2018. PGV measurements were also made along an additional array section extending up to 70m perpendicular to the track where PGV values, due to train passage, gradually decreased with distance to the track, as expected.

The number of occupied houses that are situated within 20 meters of the railroad track and therefore could potentially be experiencing the above-mentioned levels of ground motion in the Groningen province are estimated to be under 50. The number of structures, both occupied and unoccupied, that lie within ~20 meters of an operational railroad track, over the entire country is greater than 35,000. As shown in this report, the ground motion may not subside substantially for another several meters away from the track. Including buildings within 25 meters from any track, for the Groningen province the number of occupied buildings is 179, and for the rest of the Netherlands the number of all structures is close 50,000.

The observed train ground motions in this experiment were found to reach but not exceed the $3\ ^{mm}/_{s}$ threshold during the surveyed period, attesting to the feat of exceptional engineering of the train-track system. Typical frequency content of train passage is roughly bimodal: between 5-10Hz and 30-40Hz, whereas a typical Groningen earthquake signal energy starts to decrease significantly after ~25Hz. The duration of some of the longer trains, presumably freight, were approximately 40 seconds long. There is a high variability measured in ground amplitude response due a source of noise, in this case train passage, underscoring the importance of using multiple measuring stations to properly asses ground motions.

Introduction

The main objectives of this survey are to measure ground motions caused by daily non-high-speed trains and gain an understanding of the vibration levels proximal to the train tracks.

Ground-borne vibrations due to train passage are well researched and documented [3]-[8]. Although train-travel is an environmentally friendly mean of transportation, there are side effects negatively perceived by the population living near the train tracks that are due to the amplitude of the ground-borne vibrations generated by trains. The vibrations are generated at the contact between the wheels and the track and the vibration amplitude is controlled by several elements such as train weight (the heavier the train the higher the ground vibration amplitude), irregularities in the wheel roundness or rail smoothness, stiffness and spacing of sleepers, as well as train speed [6], [7]. The excitation of the ground generates two types of body waves: compressional or primary -P, and shear -S waves, as well as surface Rayleigh waves whose direction of propagation is normal to the excitation source with elliptically retrograde particle motion. It has been demonstrated by [8] that partition of the excited vibrational energy is as follows: 7% by P waves, 26% by S waves and 67% by Rayleigh surface waves. It is well known that the vibration amplitude can increase if train speed reaches the Rayleigh wave velocity of the local soil. This phenomenon has been known to occur with high-speed trains as they approach speeds exceeding the Rayleigh wave speed of the supporting soil -an important aspect to keep in mind when dealing with very slow Dutch soils.

In the Netherlands, the acceptable vibration intensity guidelines are provided by SBR, the Building Research Foundation [9], and consist of 3 parts: (A) assessing damage to buildings; (B) assessing nuisance for people: determining whether vibrations due to passing vehicles or any other source create nuisance for people exposed; (C) assessing failure of equipment.

The ground velocities and frequency content measured in this survey generally agree with the published values (example [3], [5]). Although many of the measured PGV values in the present survey exceed the 3mm/s threshold, and some are as high as 16mm/s (figure 1), analysis shows that during this experiment the train-induced ground motions do not exceed the lowest SBR guideline of 3mm/s, but regularly exceed 1mm/s threshold, commonly referred to as the lowest limit for damage caused by ground vibrations [10]. Within the observed range of train-induced PGV, the higher values of up to 3mm/s we presume are due to freight trains. The highest PGV values of the survey, ranging between 3mm/s and 16mm/s were not caused by trains, but some other urban source usually with a local source like garage doors, lawn mowing, farm-field work etc.

One of the objectives of this experiment is to make this data set broadly available and enable research groups studying train vibrations to further their investigation and aid in calibration of the numerical models.

Data Acquisition

This seismic survey was conducted along a portion of the railroad track in the Groningen province, in the Netherlands. The survey consisted of 77 3-component geophones placed in two receiver lines, one along the track with a short section at a ~35° angle to the track, and another line placed perpendicular to the track (roughly outlining a T-shaped pattern; figure 2). Densely spaced geophones, 2.5m apart, were placed 15m from the nearest track section (geophones 1 through 43), covering ~105m, followed by a 35m receiver line (geophones 43 through 56) at an approximately 35° angle to the track, and a receiver line perpendicular to the railroad of ~55m length (geophones 57 through 77), starting close to the middle of the track-parallel receiver line section (figure 2). The survey recorded ground motions

over a period of 56 days from December 2017 to February 2018. In the subsequent text, day of survey refers to the day of the year.

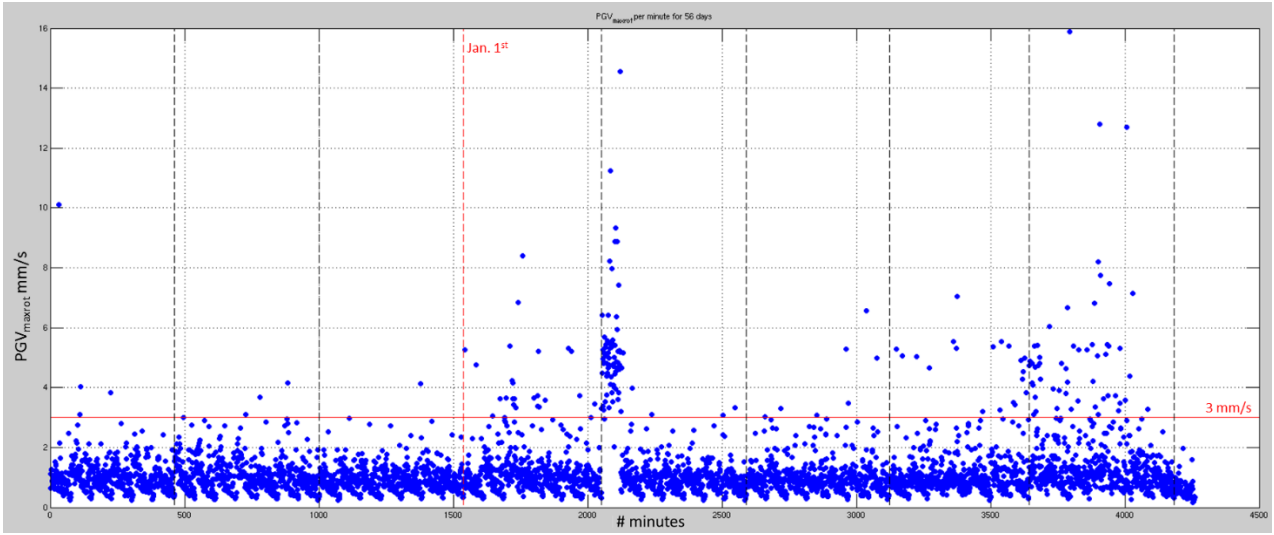

Figure 1. PGV measured per each minute of a 56-day survey for all 77 stations. Vertical dashed lines denote the beginning of each week (00:00 hrs on each Monday), with January 1st 2017 shown in red. Horizontal red line marks the lowest SBR threshold of 3 mm/s. As further analysis shows, none of the values exceeding this threshold were caused by a train. Apart from January 8th, a daily symmetry is seen in the data, indicative of daily train schedules.

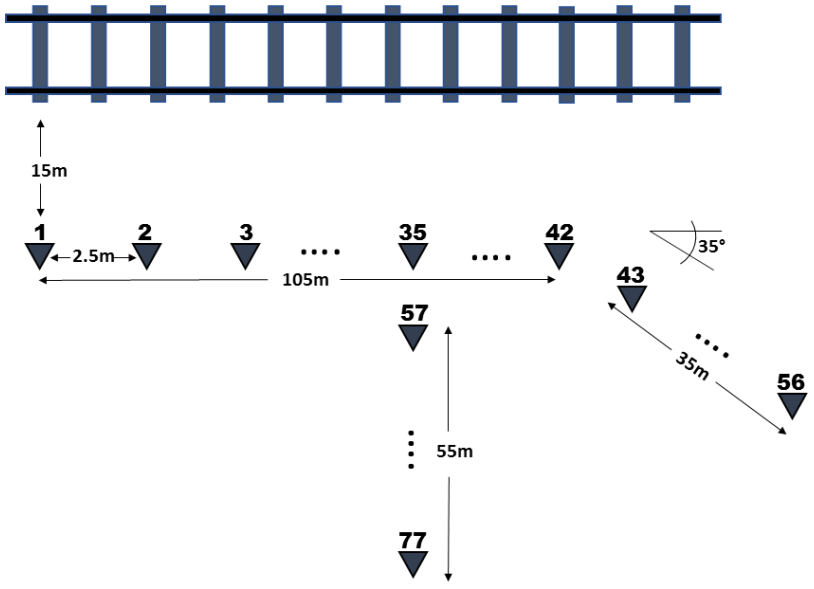

Figure 2. Schematic of the seismic monitoring array geometry. Triangle symbols represent geophones, numbered as indicated. A portion of the array follows the track at 15m separation (geophones 1 through 43), then assumes a ~35° angle to the track (geophones 43 through 56). Geophones 57 through 77 are placed perpendicular to the track, starting at geophone 35.

The geophones used were 3-component GS-one standard model phones manufactured by Geospace, recording ground particle velocity. Each geophone is equipped with three 150mm-length spikes and was buried shallowly into the ground for improved coupling. The components were aligned in vertical

and North directions. The sampling interval was 2ms (500 samples per second), with the resonant frequency of 5Hz. Data was recorded continuously on 77 3-component geophones for a period of 56 days and stored in 1-minute files in segy format (18,627,840 traces). One segy file covers a 24-hour period for one geophone station. Trace zero, refers to minute 0, the first minute of the 24-hour period starting at local midnight. In the subsequent text, terms trace and minute are used interchangeably and refer to the minute of the day of survey.

The surveyed section of the railway track is classified as at-grade (figure 3). There are other types of railway sections including embankment, cutting, or abutment site (see [5] for example). Field measurements show the vibrational effects of at-grade type of railway track on the measured ground motion are moderate, with peak particle velocities between values observed for embankment and cutting earthworks profiles [5]. The survey in this report was conducted by a third party with work consisting of installation and operation of the geophone network. As a result, the number and type of trains or their composition was not monitored and therefore not made available to corroborate the analysis herein. In fact, no additional observations beside geophone records (such as for example soil properties) were obtained during the 56-day seismic survey.

Figure 3. View of the at-grade railroad track, part of which was surveyed in this report.

Data Processing

Because geophones respond to the ground velocity in millivolts, a correction is necessary to convert the recorded samples to units of velocity, as well as compensate for the instrument sensitivity at different frequencies (instrument sensitivity: 89.4 V/m/s; damping: 67%).

Before computing the peak ground velocity, data is conditioned as follows. Each one-minute long trace is detrended and filtered with a zero-phase (acausal) Butterworth filter for reasons outlined by [11]. All traces are band-passed between 1 and 200 Hz. Two different definitions of peak ground velocity are considered in this study. First, a single maximum value is computed for all three components of motion for each minute of the survey, and the larger of the two horizontal components is kept, PGV_{Larger}. It is worth noting that in most cases the Y (North-South) component was found to be the larger of the two horizontal components and often the largest (larger than the vertical). Because geophones were aligned in the NS-EW directions while the track itself is not, PGV_{Larger} did not capture the maximum amplitude of motion. This is commonly experienced in earthquake ground motion

monitoring where the orientation of the source is seldom aligned with the orientation of the ground motion recording instruments. To work around this and compute the largest ground motion, following [12], we rotate the horizontal components and compute a PGV_{RotMax} as follows (this method is effective for rotation through small angles):

$$PGV_{RotMax} = max\left|\sqrt{V_{NS}(t)^2 + V_{EW}(t)^2}\right|$$

PGV_{RotMax} produces a greater value that any individual component, for all records in the data set, as noted by [11]. For the rest of this analysis we focus on the PGV_{RotMax} and from here on, by PGV we in fact mean PGV_{RotMax}.

Survey Highlights

To better understand the recorded signal, it is of interest to review the mechanism by which trains excite ground motions. As described in [6], a moving train exerts a series of load forces from each wheel axle onto the track, causing quasi-static pressure and downward deflection of the track. This deflection exerts pressure on all sleepers involved, which in turn apply vertical forces to the ground for the duration of the track deflection. The elastic waves that are generated by series of vertical forces have wavelengths much larger than the sleeper dimensions, such that sleepers can be modelled as point sources. Thus, a moving train is generally modelled as a moving set of point loads. The type of waves generated by train passage are body waves, primary -P and shear -S waves, as well as the surface Rayleigh waves, which carry most of the generated energy [9]. It is estimated that about 7% of the energy is carried by compression waves, 26% by shear waves and 67% by Rayleigh surface waves [8]. The speed of each of these waves is determined by the material they propagate through (in this case shallow soil) but the amplitude is in part affected by the speed and weight of the train. Other effects such as train acceleration, or exceedance of the Rayleigh wave speed can also have an impact on the ground amplitude. An example of a train signal (recorded on day 32, minute 991 or 16:31 hours) is shown in figure 4.

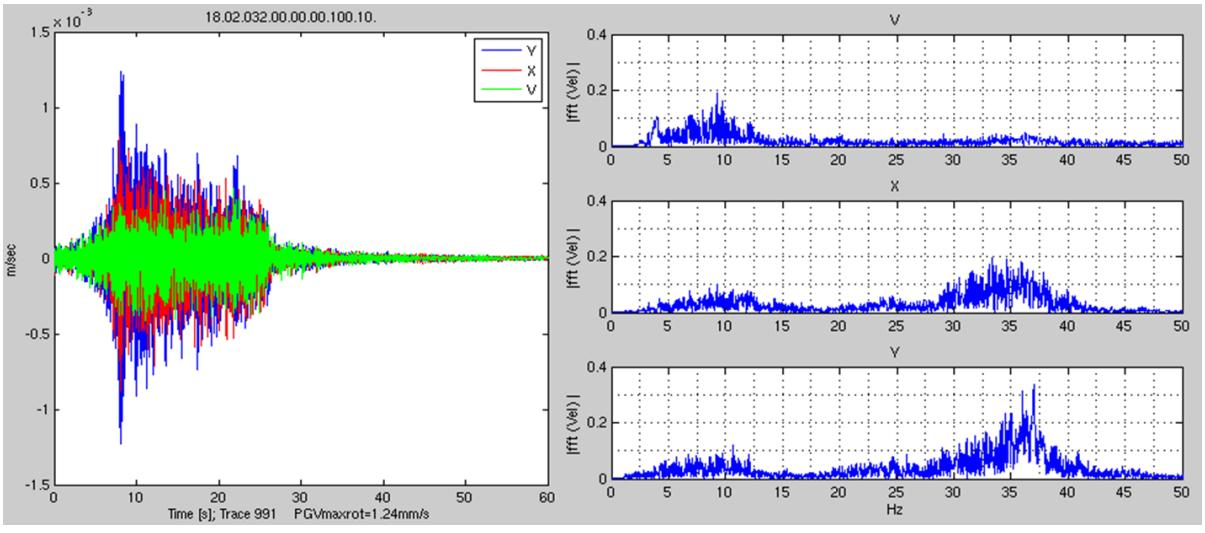

Figure 4. Example of a train signal. Left: 3-component velocity signal of train passage over 20s showing radial component Y (blue) dominating over transverse X (red) and vertical (green); Right: fast Fourier transform of the vertical V, horizontal X and Y components, top to bottom respectively. The roughly bimodal frequency content is common for train ground motions with energy around 5-15Hz and 35-40Hz.

The time duration of this train signal is approximately 20 seconds and the ground motion peak amplitude is 1.24mm/s. This example is measured on geophone #10, and as will later be shown, there is a fair amount of variation in peak ground velocities from station to station for a single train. Given this duration and a relatively high PGV, we presume this signal to be from a freight train.

Interestingly and perhaps unexpectedly we find that the largest ground motion is in the radial-Y component direction, and the lowest vibration to be in the vertical direction for this example as well as most of the train signal inspected. We note that [5] find the vertical vibrations to be the dominant ones for the first 35m from the track beyond which the vertical and horizontal vibrations equalize. The present survey was done at 15m distance to the nearest track as well as the perpendicular line spanning an additional 55m (in total, covering ~70m distance from the track), and the vertical component was seldom found to be the dominant one.

The three-component frequency content reveals a bimodal energy distribution between roughly 5-12Hz and 30-40Hz. This general pattern agrees with that discussed in the literature (for example figure 5, adapted from [5]). The combined effect of the bogie passage and car bogie bounce, seen on all three components, is the largest in the vertical direction with energy observed between 4 and 12Hz, while the effects of wheel passage, wheels out of roundness and upper soil Green's function are seen on both horizontal components and slightly higher on the Y-component around 37Hz. There is essentially no energy arriving at frequencies beyond 50Hz, ruling out contributions of the lower portion of the list items on y-axis in figure 5.

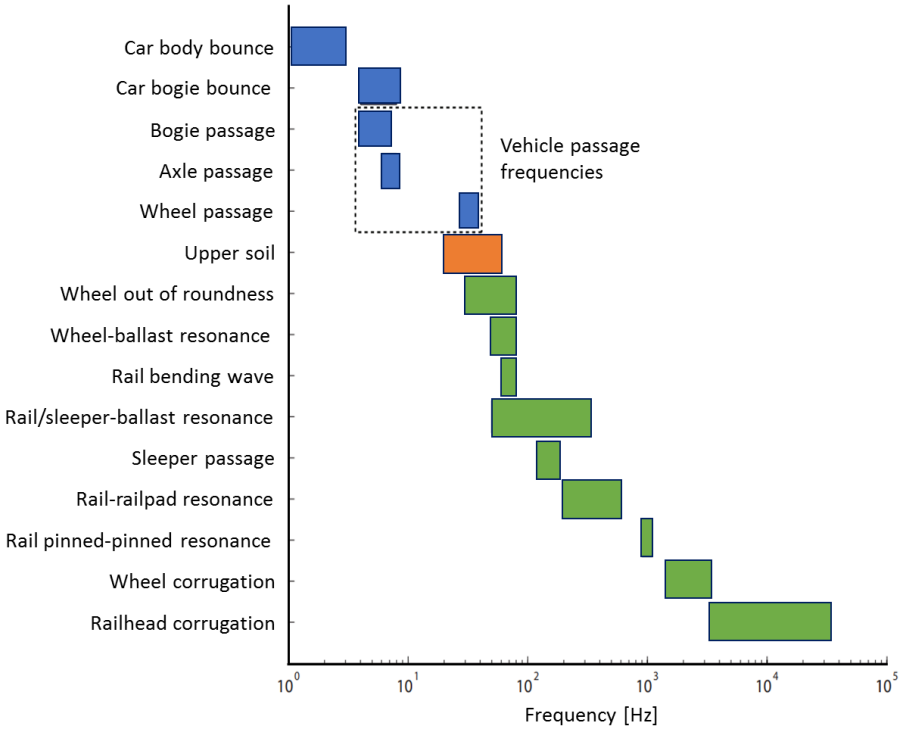

Figure 5. Figure adapted from [5] illustrates frequency content of various train-related sources. The frequency gap outlined by a dashed box is observed in this survey.

Max PGV and Comparison to SBR Guidelines

PGV was computed following a method discussed above for each minute of the 56-day recording campaign (figure 1), and for each component of all 77 3-component geophone stations in the array. PGV_{RotMax} represents a combination of the horizontal components. Given the roughly T-shaped seismic array geometry, the train-to-station distance in figure 2 varies; also, the railway track spacing between the near and the far tracks has not been accounted for. Nevertheless, this type of representation provides a useful quick way of assessing the levels of top ground velocities and spotting anomalies. An example of such an anomaly is observed on January 8th, date coinciding with that of the third largest induced earthquake in the Groningen field, discussed in the following section. Analysis of this anomalous behaviour confirms it is not related to the earthquake but rather caused by an unknown urban source (discussed in section Day 8 Amplitudes).

One of the objectives of this survey was to compare all measured PGV's to the lowest SBR building vibrations guideline of 3mm/s. Because the max PGV computation is performed each minute of the survey, over the entire data set the lowest SBR threshold has been reached or exceeded 189 times (figures 1 and 6).

Although some of the PGV values observed in this survey reach nearly 16 mm/s, further analysis of each of the traces with PGV values exceeding 3mm/s shows they are some sort of a local disturbance of short duration (few seconds) and have an unambiguously different frequency content compared to that of a train passage signal. The signal is often localized or confined to a few neighbouring geophones and is observed in no more than a few traces (i.e. a few minutes during which short bursts of amplitude exist). The high level of noise is found on geophones positioned closer to the buildings such as a garage, shed, a house, or next to the walkways. We label those signal traces that exceed the 3mm/s threshold "other urban noise" to indicate that the source is man-made but not fully identified. Examples of those velocity traces and their corresponding frequency content are shown in the sections below.

The observed train ground motions reach the 3 mm/s threshold during the surveyed period. We presume this is due to the heavy freight trains.

Thus far we have focused on the 3mm/s SBR vibrations threshold. However, a vibration threshold of 1mm/s is commonly regarded to as the lowest limit for damage due to vibrations and is used by TNO to trigger an in-person damage survey of houses that have experienced that level of vibration from induced earthquakes in Groningen [10]. The number of instances where the 1mm/s threshold has been reached or exceeded during the survey in the present study is 1,913 times (figure 6) for the entire data set. Here we note that the large volume of this data set was not conducive to the individual analysis of every single minute-long trace, thus not all the exceedances are due to train passage. A more focused data set includes removing day 8 anomalies and station 4 recordings (reasons discussed in later sections) as well as all the perpendicular array stations (geophones 57-77) where amplitude has been observed to decrease. The resulting subset then represents the PGV values experienced along the track with any false highs removed. Out of those PGV values, the 1mm/s threshold is exceeded 711 times over 56 days, along a 100m stretch.

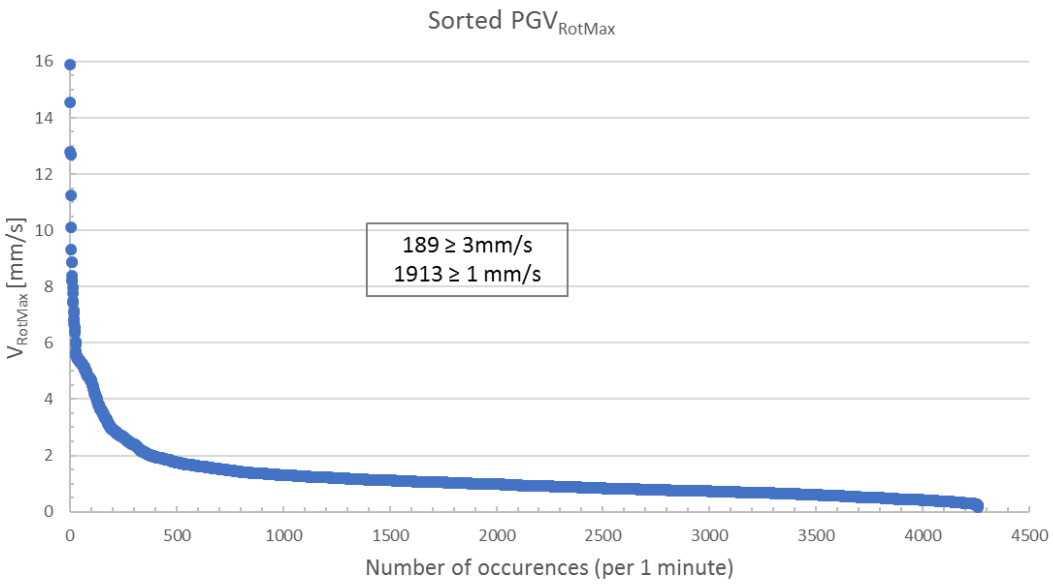

Figure 6. Sorted PGV per minute of the 56-day survey. 3mm/s SBR threshold was reached or exceeded 189 times, while the commonly set 1mm/s damage threshold has been reached or exceeded 1,913 times.

Benchmark: Zeerijp M3.4 Event

The present study seismic survey was operational at the time of the third largest earthquake in the Groningen field, the M3.4 Zeerijp event of January 8th, 2018. The largest two earthquakes in the Groningen field thus far were M3.6 Huizinge event of August 2012, and the M3.5 Westeremden earthquake of August 2006. The recent M3.4 Zeerijp seismic event was recorded on the entire T-array (figures 7 and 8) and presented a unique opportunity to benchmark the ground motions recorded by the instruments. In the future, this dense data set could be used to augment the existing earthquake records and perhaps aid in analysis of a range of seismology topics of interest to the academic groups. The Zeerijp event was well recorded on the extensive local KNMI network, the official network responsible for detection, location and magnitude determination, among other parameters, of all local earthquakes [13], [14].

A shot-gather of the Zeerijp event shows nicely the P and S phase arrivals (figure 7). The identical arrivals times across the entire array (figures 6 and 7) indicate a relatively large distance to the source (~30km). In contrast, a train passing by the array on the nearby track is recorded with a different time delay at each station as seen in figure 21, depending on the direction of train travel as well as train speed. The amplitude of all the Zeerijp event arrivals is consistent throughout the array which also indicative of a large distance to the earthquake epicenter. In contrast, a train passage produces a decaying amplitude over the perpendicular section along the array as distance to the track increases (example figure 18, stations underscored by a red line).

A double-peaked P arrival is prominent in figure 7, followed by a more complex set of somewhat smaller amplitude arrivals. Slightly noisier traces around station 50 are recorded by geophones placed along a widening in the canal. A lot of complex Zeerijp earthquake arrivals beside just P and S are seen in this dense seismic array, to our knowledge the densest seismic recording of this earthquake.

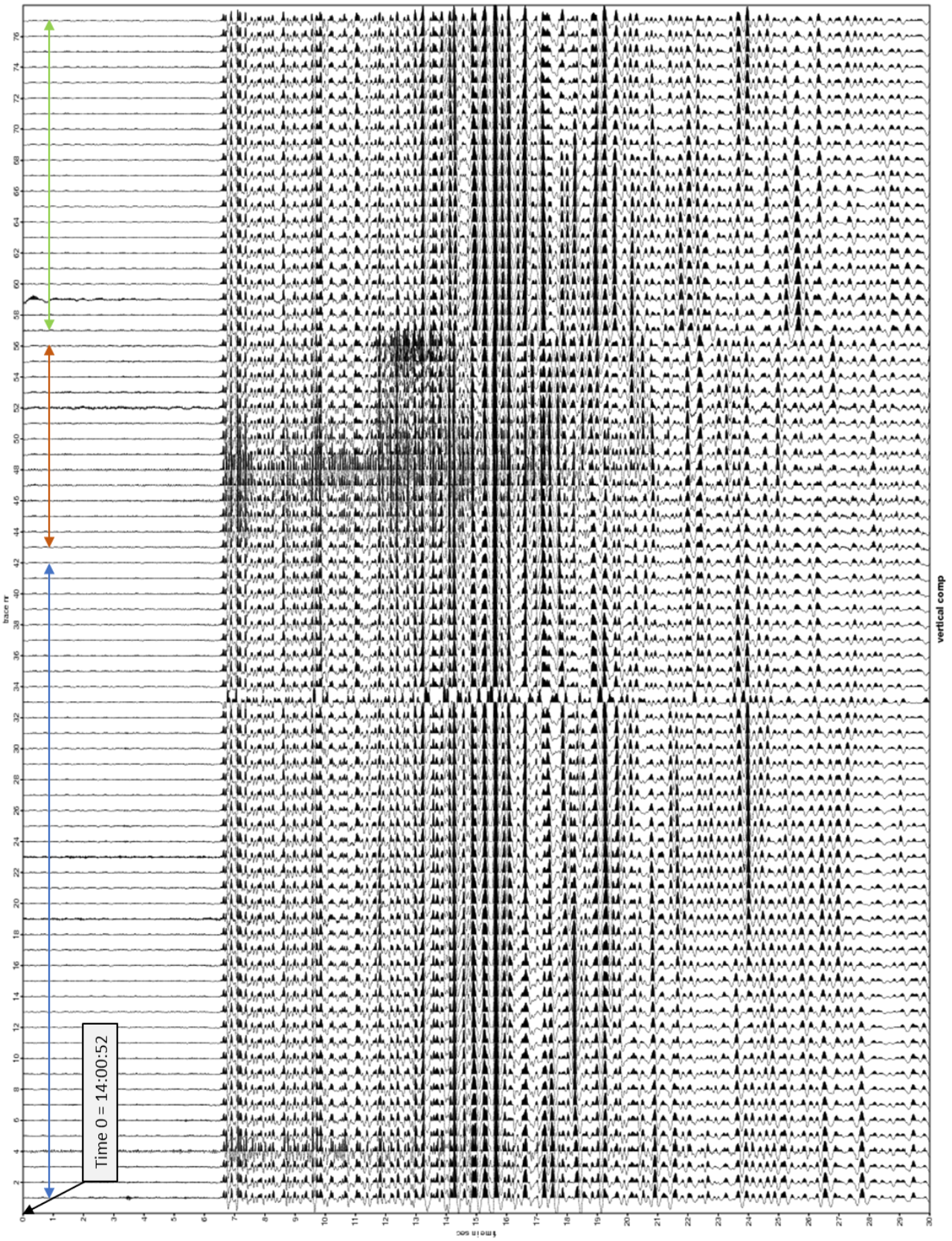

Figure 7. M3.4 Zeerijp earthquake recorded on the entire array, here showing the vertical component. Color arrows indicate geophones along the track at 15m offset (blue), array section at 35deg to the track (orange), and the array section perpendicular to the track (green). Zero time is set to event origin time.

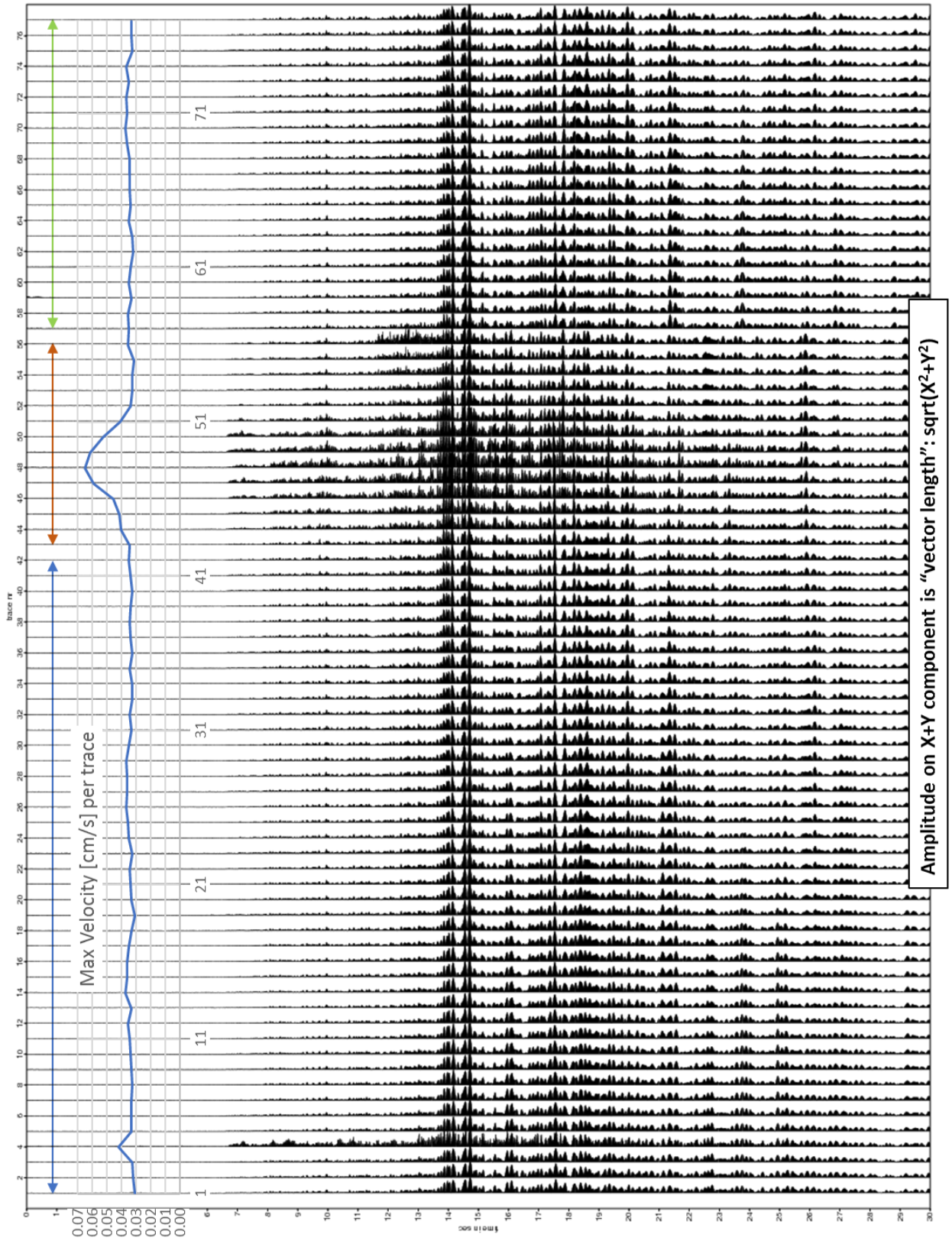

Figure 8. Same as above figure only component of motion shown is square root of the sum of squares of the two horizontal components. Computed PGV compares well with independent analysis by [13].

Maximum horizontal velocity computed as the square root of the sum of the squares is 0.6mm/s. This value is within the range of calculated PGV values by [13], who make an observation that the motions recorded for this earthquake are broadly consistent with the predictions from the ground motion model that is currently deployed in the seismic hazard and risk modelling for Groningen.

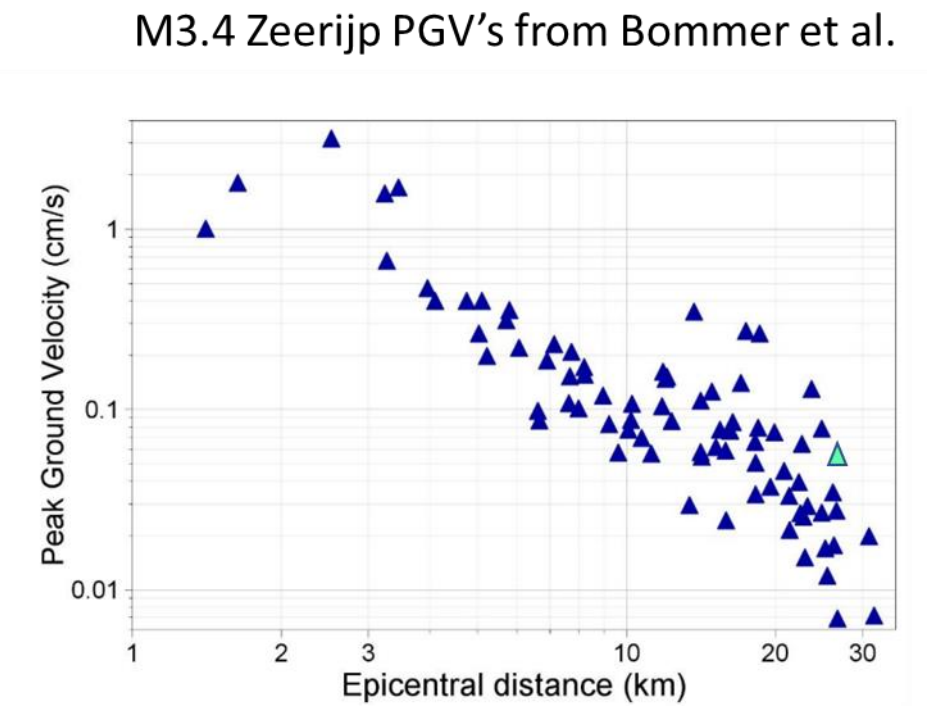

Figure 9. Figure from [13]. Jan. 8, 2018 Zeerijp M3.4 earthquake observed by the surface KNMI network. The T-array was located around 30km from the Zeerijp epicenter. Green triangle indicates the PGV computed for the Zeerijp event in this study.

Spectral analysis of the Zeerijp earthquake signal shows an overlap in frequency content between the earthquake and the train signal (figure 9). For this comparison a daily commuter train signal was selected (type of train is presumed due to a short signal duration, time of occurrence -midday, and an average PGV value). The two different signal spectra overlap in the 5-10Hz range, although the earthquake has a larger amount of energy in the lower end of the frequency range, below ~5Hz, while the train spectrum has a slower spectral roll-off at higher frequencies (figure 9). The lower end of the frequency range is potentially more damaging to buildings, thus the threshold levels vary with the frequency range as stated by [9], [10]. It is interesting to note that a daily commuter train causes higher amplitude of ground motion than one of the largest earthquakes in the area, at an epicentral distance of ~30km (figure 10). Some of the heaviest trains recorded in this survey caused ground motions of 3mm/s, measured up to 20-25 meters of the train track, on a weekly basis (and at times even daily). These graphs would suggest that experiencing ground motions from an everyday train is not dissimilar to residing within ~5km of one of the largest earthquake in the Groningen field.

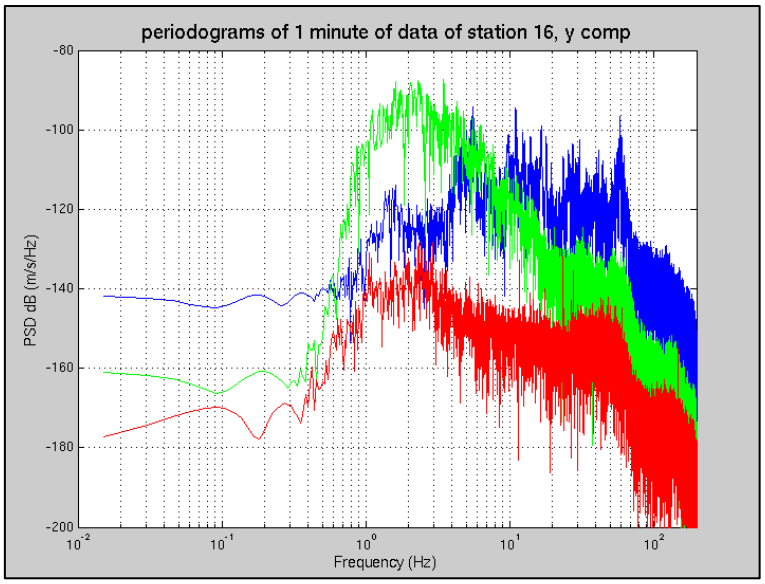

Figure 10a. Periodograms: Zeerijp earthquake (green), a commuter train (blue), and background noise (red).

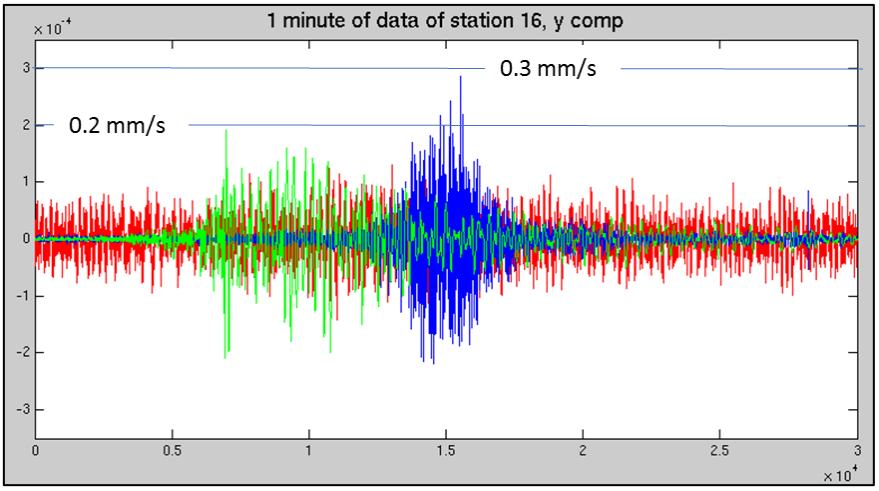

Figure 10b. Velocity traces of a train (blue), Zeerijp earthquake (green), and background noise (red). At 30km from the epicenter, Zeerijp earthquake amplitude is lower than a local commuter train. The time series for all three signals are shown in samples (at 500 samples per second sampling rate).

Day 8 Ground Motions

Analysis of the peak ground motion per 24 hours are an informative and quick scan of the data set. In the present survey example, daily peak motions are roughly repetitive in value, indicating daily train schedules, except for January 8th (figure 1) coincident with the date of one of the largest earthquakes in the region, M3.4 Zeerijp event, with the epicenter located approximately 30km to the North-East of this seismic array. The earthquake itself was recorded by the array and as already discussed, its PGV computed to be in general agreement with the observations by [13]. Thus, the unusually high PGV's for this day (figure 11) motivated a further inquiry into data. The timing of the day-8 peak values (~08:00) was several hours ahead of the time of the earthquake (~14:00), meaning there is no causality between the earthquake and the observed high ground motion amplitudes. Further, the timing (or moveout) of the peak PGV values along the monitoring array shows a speed of approximately 0.3km/h (figure 12).

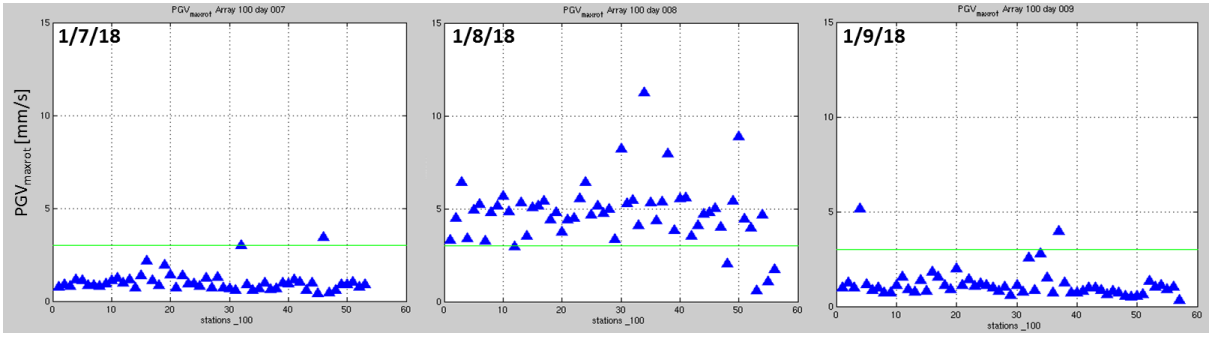

Figure 11. Daily maximum PGV's recorded along the railroad track for three consecutive days show January 8th values are higher than the other days (also, figure 1 for comparison with other survey days). Further inspection shows anthropogenic, non-train source causing vibrations around 0800hrs.

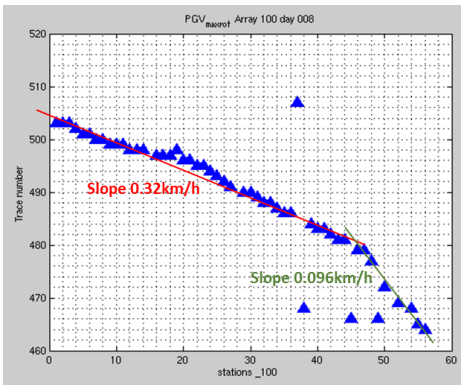

Figure 12. Time of occurrence of the highest PGV on January 8th, shows a speed of 0.3km/h. The change in slope along stations 43-56 is likely a result of the array geometry and position relative to the track.

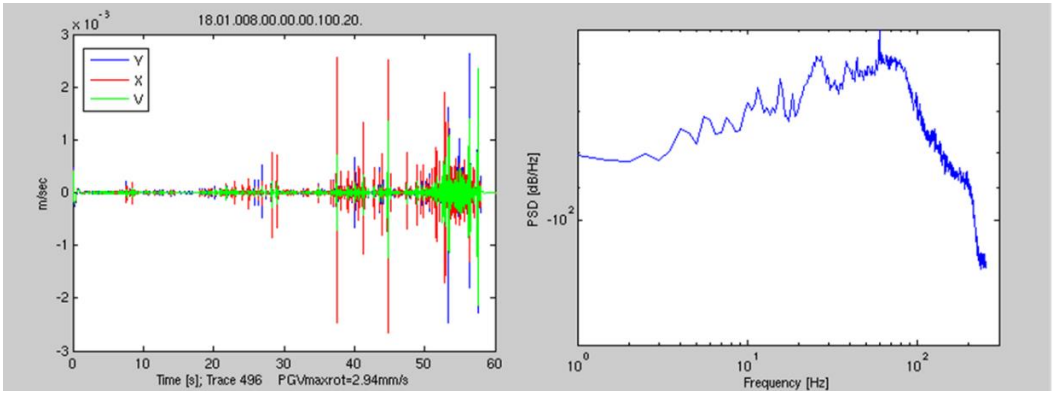

Figure 13. Example of the high PGV signal on the morning of January 8th, here shown on station 20. The same signal is observed at other stations with a moveout of ~0.3km/h between stations 1 and 42, and a slower moveout of ~0.1km/h between stations 43 and 56. Left: time series of the spurious high amplitude signal with a 3mm/s PGV; Right: Power spectral density of the time signal.

Because of the apparent change in the signal speed from 0.32 km/h for the first 42 stations, to 0.096 km/h beyond station 43 (figure 12) where there is a body of water abutting the track causing the effective break in geometry of the seismic array, we conclude the ground noise likely originated on the

other side of the track. Judging from both the time domain and the frequency content of the traces this signal is a non-train source (figure 13) and seems consistent with a slow walking pace along the track while performing some type of field work, etc.

Other examples of unknown sources of high ground velocity show signal that repeats every half a second or so, lasts less than a minute with 40Hz bursts of noise (figure 14).

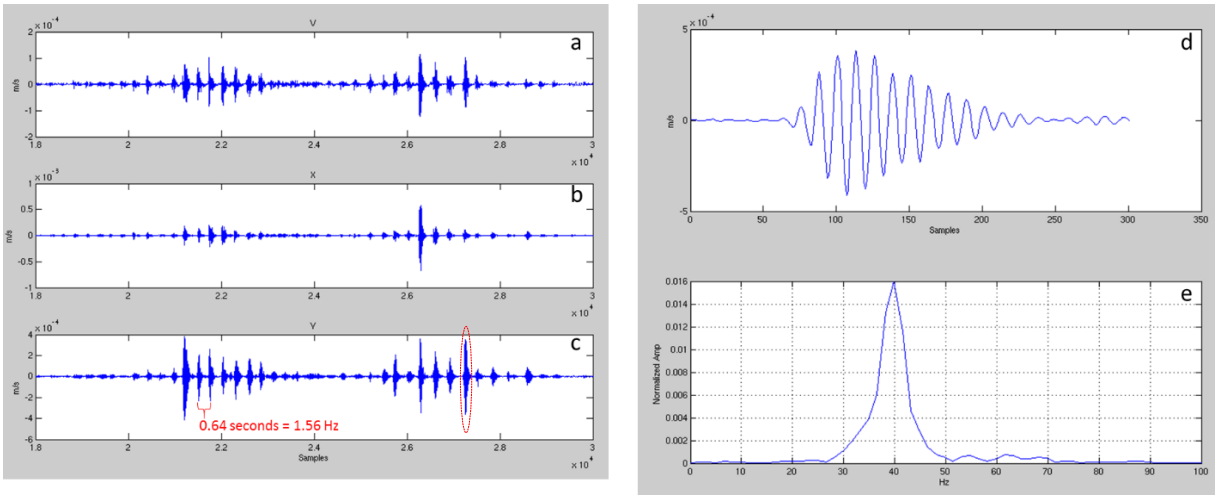

Figure 14. Signal recorded on day 33, station 35, trace 489 is an example of urban noise. Three individual components of motions of the signal are shown in a, b, c, over 1 minute; the signal marked by a red dashed oval is shown in d, with its corresponding frequency content in e showing a peak at 40Hz.

A comparison of high amplitude signals with that of train passage (figure 15) exemplifies the unambiguous difference in the ground motion, in the overall signal shape and its duration as well as frequency content: non-train noise in this example peaks at 40Hz whereas a train has been shown to have a recognizable double-peaked frequency signature in the roughly 5-10Hz and 30-40Hz frequency bandwidths. Signals such as the ones shown in the top three panels of the figure 15 account for nearly all of data points that exceed the 3mm/s ground vibration threshold shown in figure 1. As noted earlier, during this survey no other information was recorded apart from the ground motion discussed, prompting us to speculate on the origin of the other urban noise sources. The recent report by TNO [10] validates the relatively high ground motions seen in this survey with their own data from private homes where additional information of specific daily activity detail was provided by the owner. For example, 10mm/s can be caused by nearby traffic, and 2.2mm/s by dropping an object. Thus, the proximity of buildings (house, garage, shed, etc.) or walkways to any of the geophones in this survey is consistent with the type of (non-train) signal observed as well as the amplitudes.

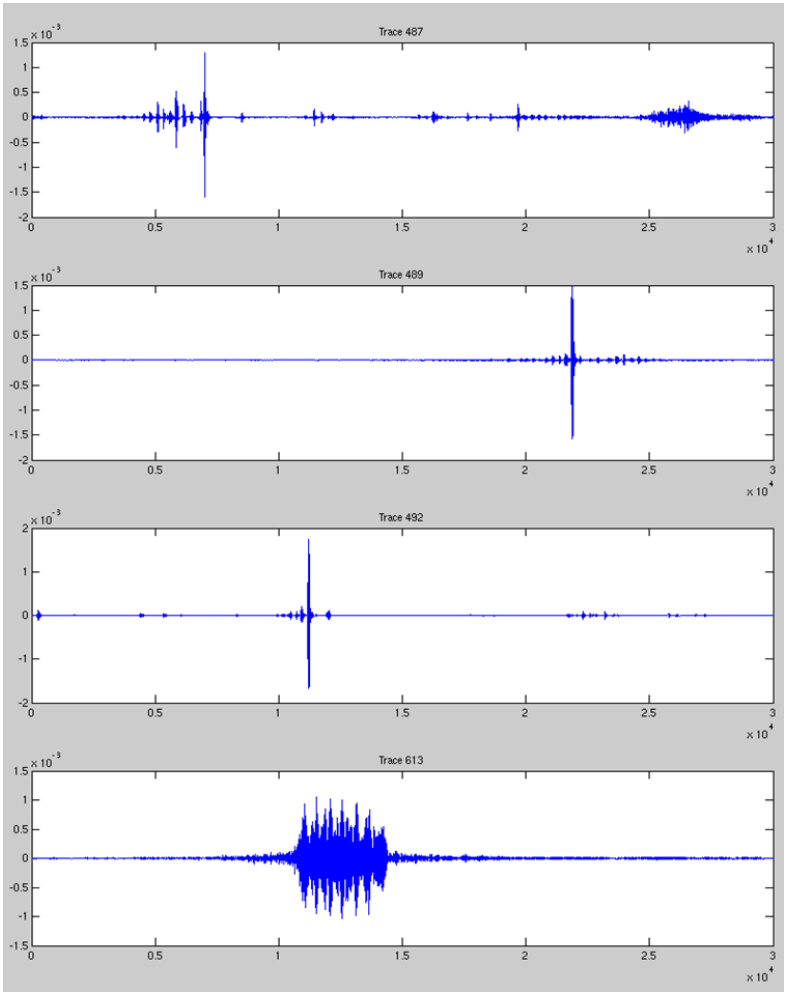

Figure 15. Comparison of train (top 3 panels) and non-train (bottom panel) high amplitude signal; y-axis is in mm/s; x axis in samples (500 samples per second).

Station 4 Anomalies

Through computation of the peak ground motion values throughout the survey, it became clear that station 4 recorded anomalously high ground velocities. Some of the highest PGV's in the entire survey were recorded on this station at nearly 13mm/s. When the daily maximums for all 56 days were compared with the neighboring stations 3 and 5, only 2.5m apart, it was evident that station 4 was recording values several times higher than its neighbors (figure 16). An example is a train signature from day 32 apparently causing 11.3 mm/s ground motion on station 4 (figure 17). The first half of the raw train signal was clipped, and the corresponding velocity signal shows an odd amplification and low frequency, with the apparent triangular shape likely being an artefact of the filtering.

Station 4 stopped recording for a total of 6 hours that day and the station clock was out of sync which made it impossible to find out what minute 99 corresponded to on other stations. Thus, we were not able to verify this train signal on other stations on that day. For the remainder of the analysis we effectively ignore station 4 measurements (they might be included in the figures but are not considered in any discussions).

The fact that something went wrong with a single metering station (in case of a geophone it could be a variety of reasons including calibration settings, or the installation and coupling, etc.) is reality

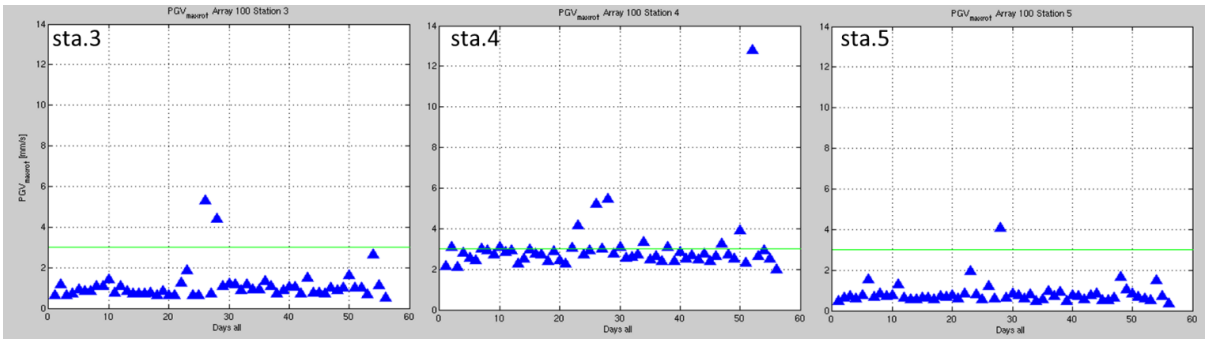

Figure 16. Comparison of highest daily PGV for all 56 days of survey, for three neighboring stations (geophones 3, 4, and 5, left to right; 2.5 meters apart) indicates unusually high values recorded by station 4.

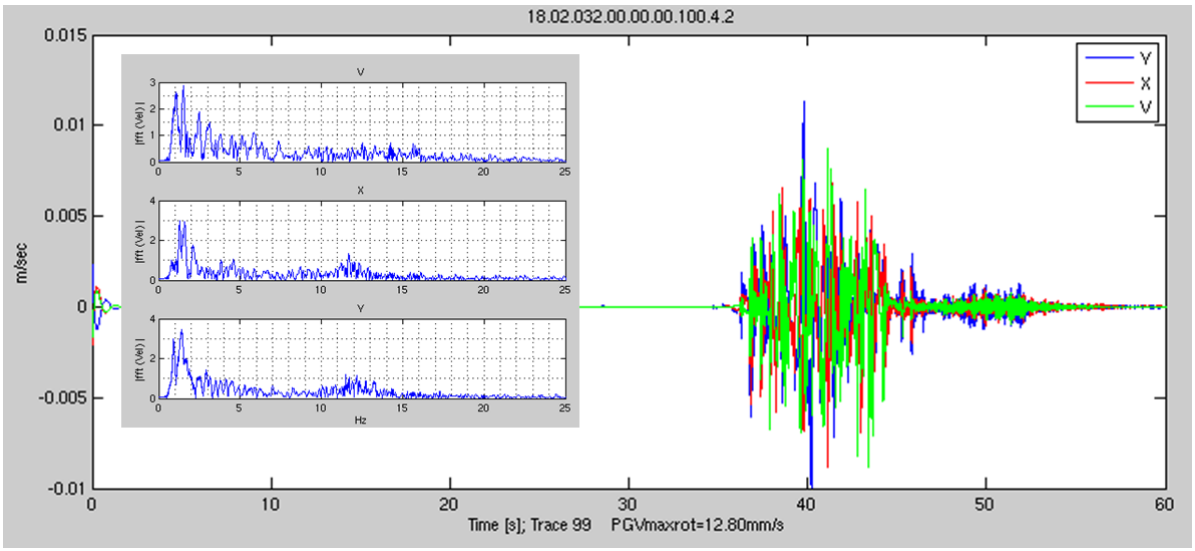

Figure 17. Example of a problematic signal on station 4. First half of the train signal appears to have a much higher amplitude and a lower frequency content (inset) than then second half.

when performing any type of field data acquisition and underscores the importance of having multiple observation points or instruments. Examples include monitoring ground motion with accelerometers, geophones, tiltmeters, etc.

PGV Variation Between Stations

A significant amount of variation is found in measured PGV for one train passage station-to-station (figure 18). This is an interesting finding since the geophone stations in this survey are only 2.5 meters apart, covering approximately 105 meters of along-track section (stations 1-42 are truly along-track, while stations 43-56 assume ~35° angle to the track). We observe that the higher the recorded PGV (likely from a heavier train) the higher the variation. Stations along the track record higher ground velocities and exhibit much higher variation than stations perpendicular to the track, as expected when distance to the source increases. Assuming all stations operate identically (apart from station 4 as discussed), the presence of the same source of ground motion, in this case a train, implies that the propagation path and site effects must amount to the observed variations in PGV. This kind of variation in peak ground motion is also seen in the earthquake ground motions and is subject of existing research.

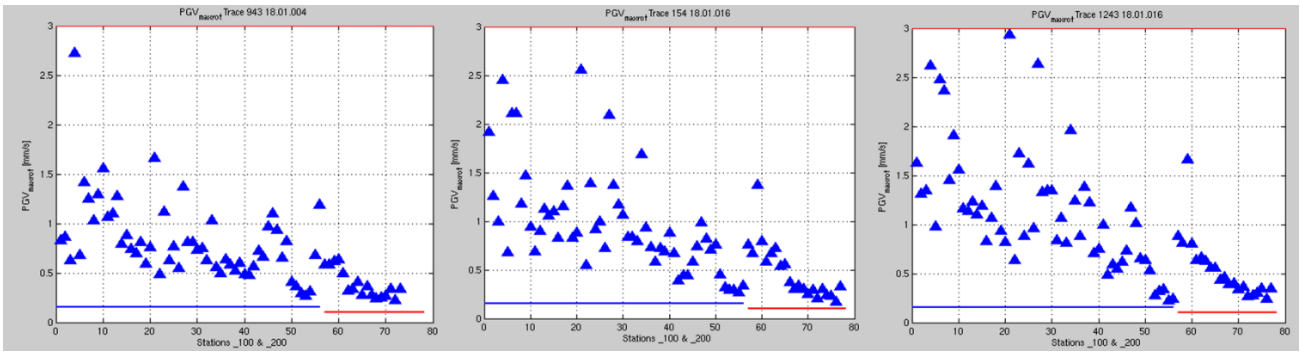

Figure 18. Variation in PGV for a train observed along the seismic array. The x-axis shows the geophone number; blue line outlines the stations along the track: 15m offset for stations 1-42, and a linearly-increasing offset for stations 43-56; red line indicates the stations perpendicular to the track. The three panels show three different trains.

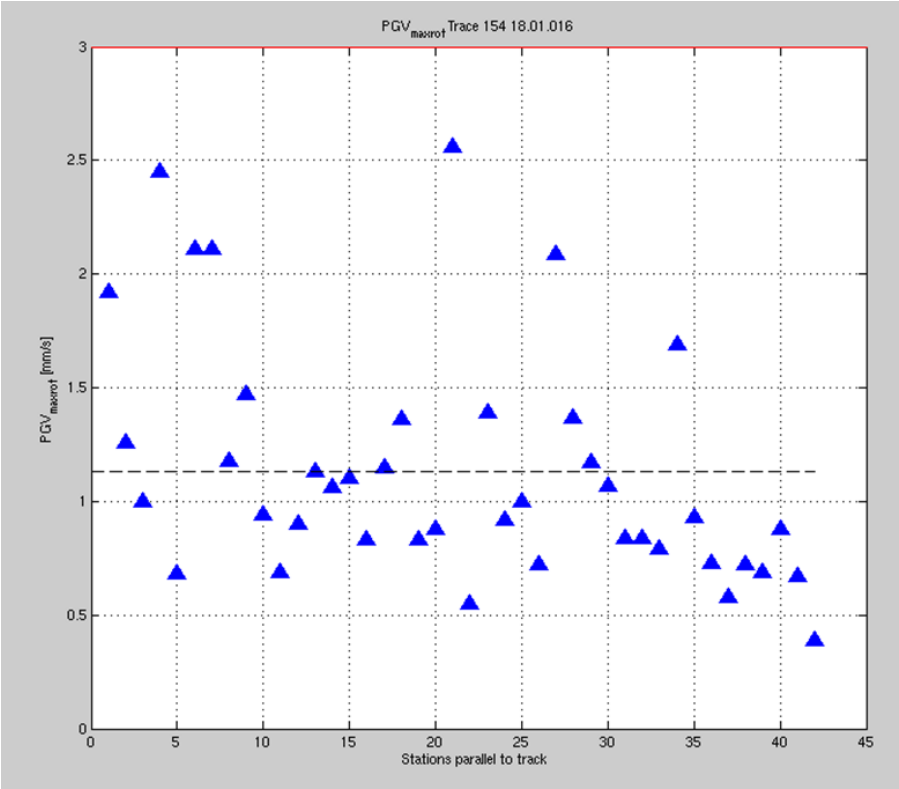

Figure 19. Same train-passage as the middle panel in figure 18; x-axis showing only stations parallel to the track (stations 1-42, all at 15m offset). The mean PGV is 1.13 mm/s (dashed line) and standard deviation is 0.52.

Train Speed Estimation

Determining the speed of a train from seismic data is not trivial because of the lack of a prominent arrival such as a P or an S wave as is the case with earthquakes. A typical train time series shows a gradual increase in amplitude, lasting the duration of the train passage (roughly; figure 20). Although a moveout (i.e. time delay) is obvious in figure 20 between stations 5, 35 and 50, station 5 evidently being the first to "hear" the train, it is clearly difficult to pin down any specific feature in the time signal since it changes in amplitude and the overall signal shape from station to station. This variation is

mentioned in the PGV variation discussion above. Relying on just the individual traces is not conducive to computing the train speed with certainty.

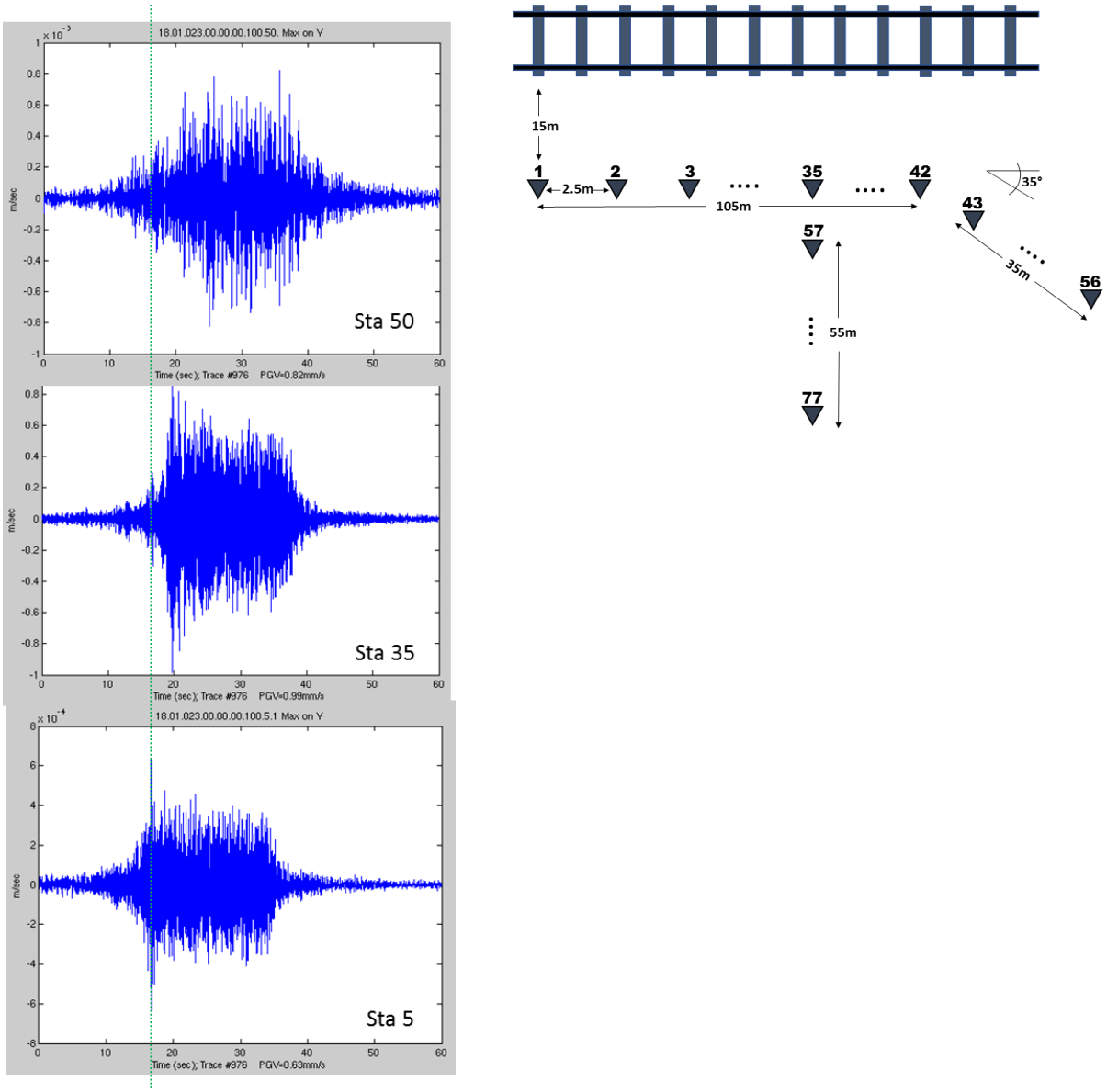

Figure 20. Example of a delay in train signal arrival between stations. This train is travelling from station 5 toward station 35 (i.e. from left to right in the schematic). Example illustrates difficulty in estimating train speed from time series train data due to a lack of clear first arrivals.

We find that a valuable way to represent the train arrival data is to plot a shot-gather, commonly used in the analysis of passive seismic data (figures 21 & 22). Two different trains are shown in the examples below. In the first example (figure 21) the beginning and the end of the train passage are clearly visible, as well as a set of faster arrivals (in white), likely the Rayleigh waves arriving ahead of the main train signal. As a reminder, Rayleigh waves are generated in the soil by the deflection of the track due to the train weight and speed. These lower amplitude waves have an estimated speed of ~200 m/s, in agreement with the shallow borehole V_S estimates near this survey as published by [16].

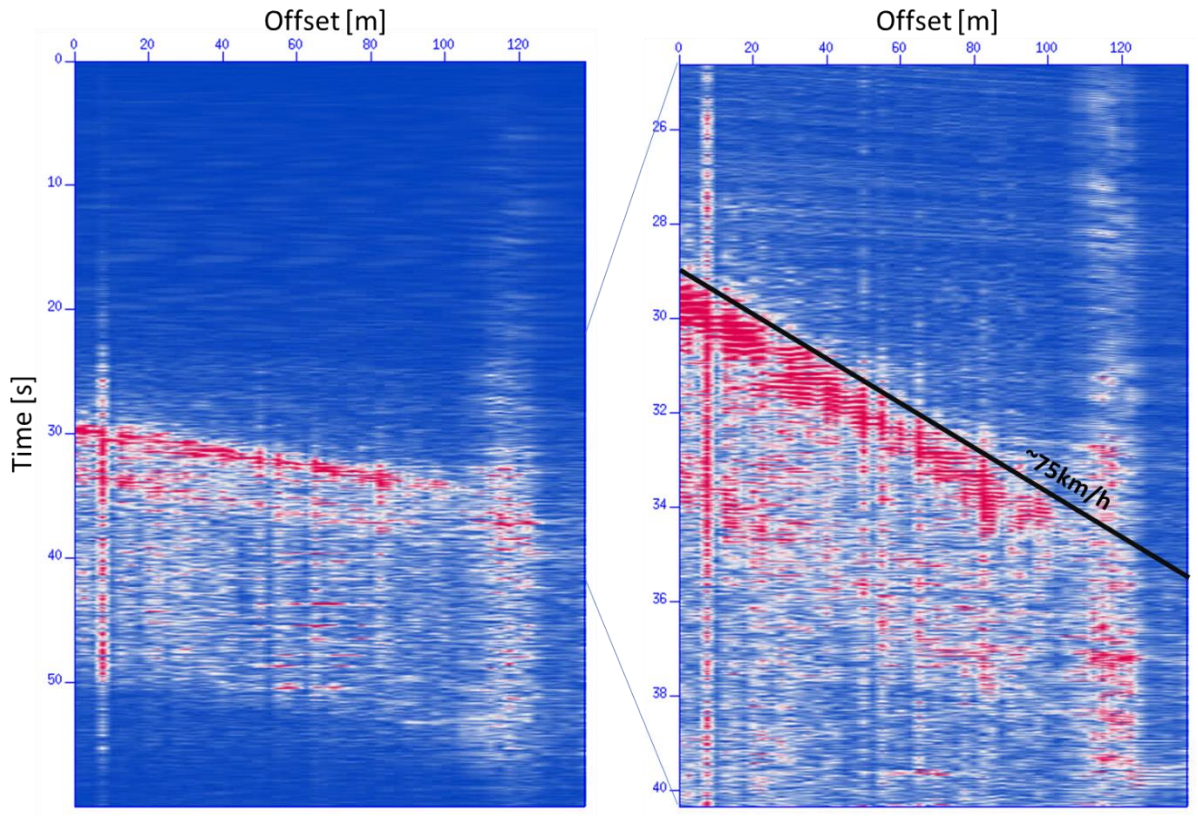

Figure 21. Shot-gather of a train signal (left) and zoom-in (right); black line highlights the high amplitude moveout; estimated train speed is ~75 km/h; problematic amplification on station 4 is evident.

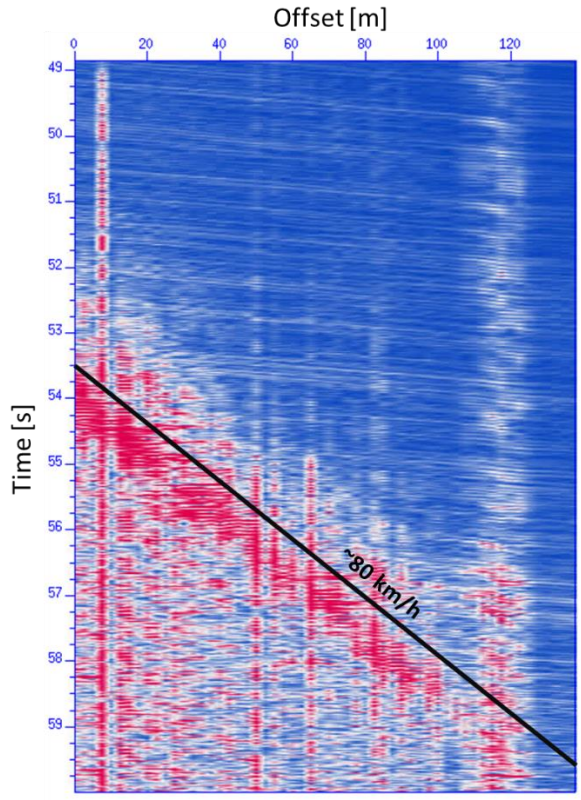

Figure 22. Shot-gather of another train signal. The train velocity is estimated around 80 km/h (24m/s). Parallel arrivals (white) captured across the array are probably Rayleigh waves arriving ahead of the train.

Ground Vibration Nonlinearity

Shot gathers as well as individual traces reveal interesting amplitude non-linearities in ground motion. A high amplitude response is observed at the beginning of the train signal for a train shown in the shot-gather in figure 21. Specifically, stations 9-12 show a high amplitude response at the beginning of the train signal, and the amplitude subsides for the rest of the trace. That response is different than at, for example, station 21 where the amplitude of the entire time trace (seen as a series of red bursts in figure 21) appears more or less equal. Similarly, stations 15, 16 and 17 respond with an even amplitude for the duration of the train signal. Another example is shown in figure 23 (train 1029, day 03) with high signal response variances observed station to station (by a factor of 3), as well as within each trace (for example at station 10). The frequency content remains broadly similar with a prominent peak at ~36Hz. Further research of nonlinear amplitude response with such closely spaced stations could have important implications on our understating of the heterogeneity in the soil response.

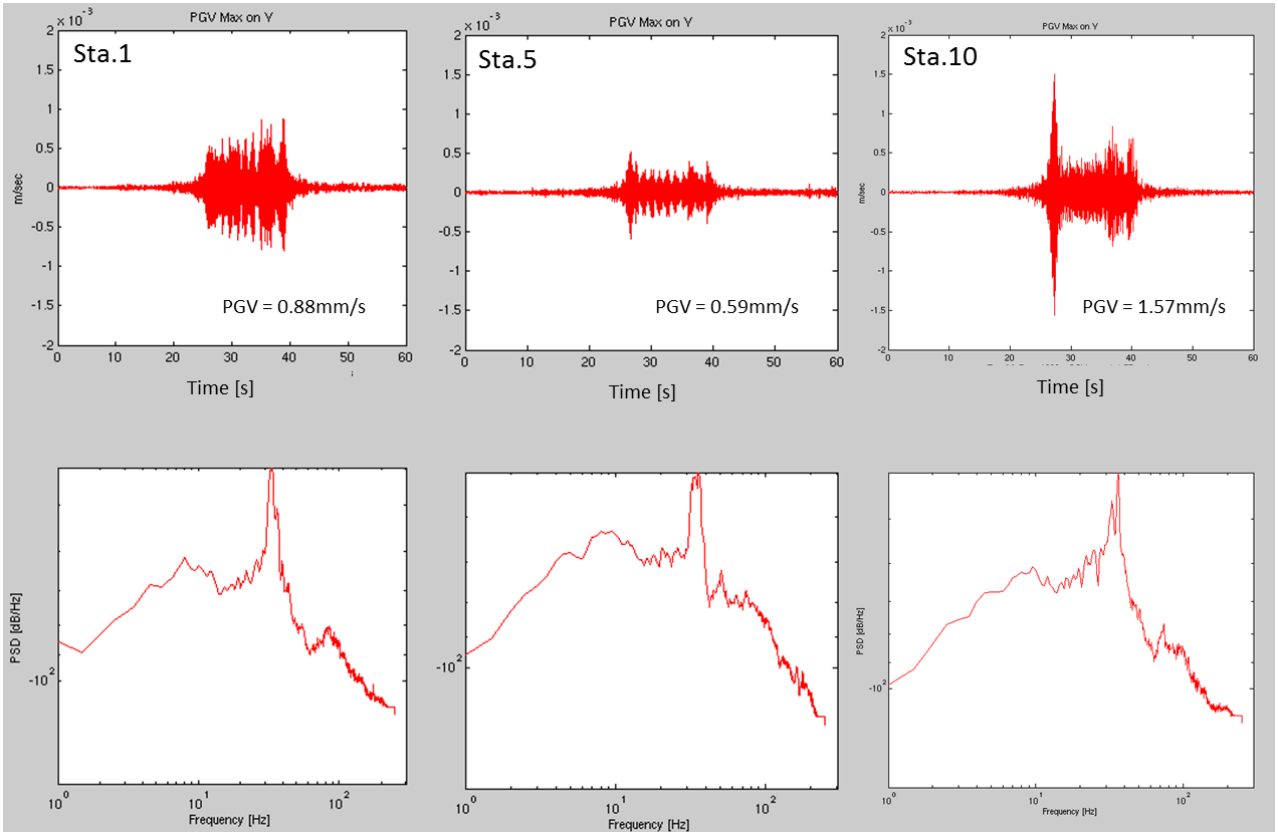

Figure 23. Examples a varying amplitude signal due to a single train across three stations 1, 5, and 10, the latter showing a prominent arrival at the beginning of the train signal. Horizontal Y component shown.

Observation of these interesting high amplitude arrivals sparked an interest in exploring the question of ground vibration boom. The effects of ground vibration boom due to high-speed trains are well documented (examples [6] and [7]). The effect of ground vibration boom is similar to the effects of focusing of sound waves radiated by an aircraft under the conditions of sonic boom. The effect of focusing of Rayleigh waves may occur if the train speed becomes higher than the Rayleigh wave velocity in the supporting soil. In the example of a moving train under the condition of ground vibration boom, a localized increase in ground vibration amplitude may be observed.

Rayleigh wave speeds in the slow Dutch soils can be as slow as 30-40 m/s or 108-144 km/h [17] and could plausibly allow for the condition of the “ground vibration boom” [6], [7] for trains travelling at speeds faster than the Rayleigh wave. The estimated train speeds observed in this survey vary from

70km/h to 90km/h or so, slower than track operating speed of 140 km/h [15]. Local surface velocity data from the soil velocity profiles taken from the nearest measurements to the seismic array in this study [16] show top soil Vs velocities of ~200 m/s (720 km/h). These Rayleigh wave values agree with the analysis of shot-gathers of the train passage data (figure 21), where the thin white lines likely show the Rayleigh wave arrivals throughout the array at the estimated speed of approximately 200m/s.

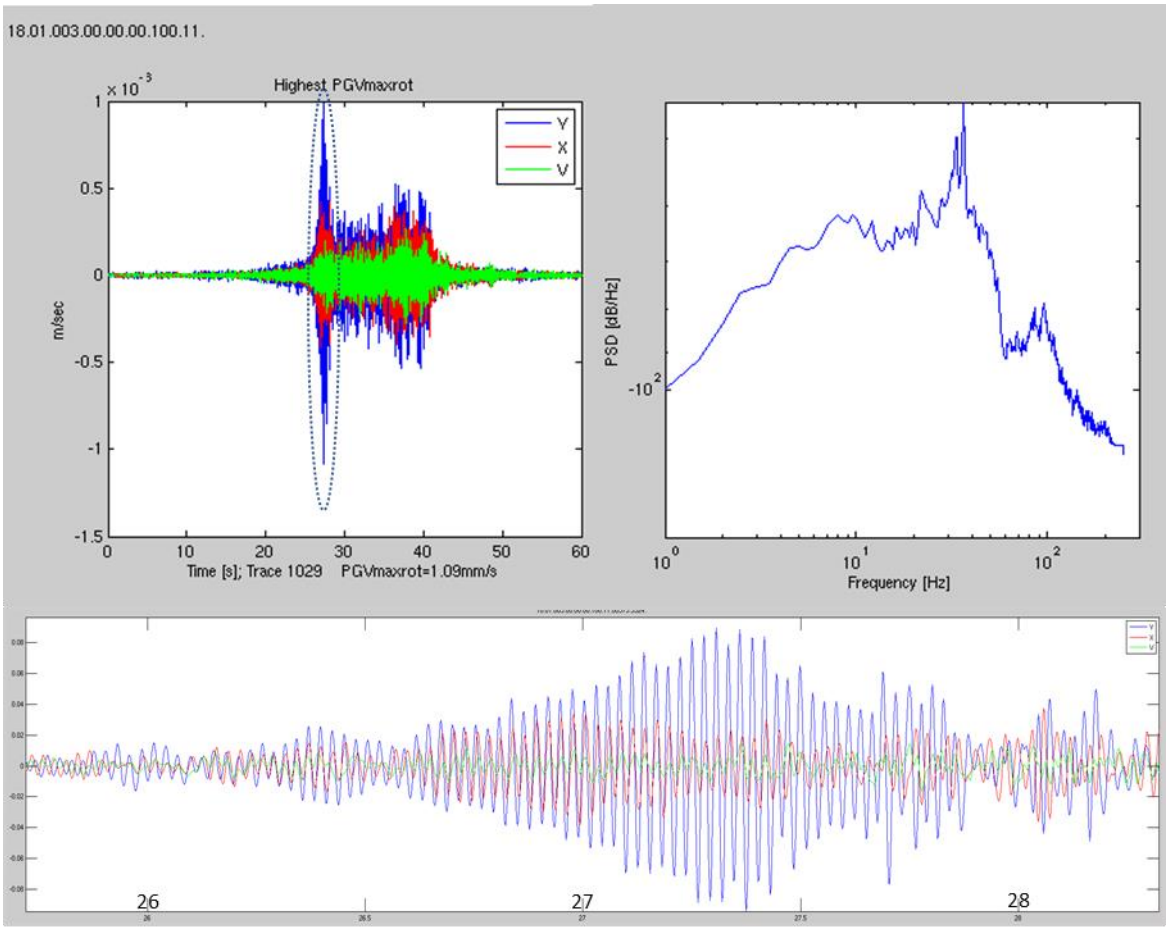

Figure 24. Top left: high amplitude arrival at the beginning of the train signal recorded at station 11; Top right: power spectral density of the entire trace. Bottom: dashed line-circled signal; duration ~2 seconds .

The relationship between Rayleigh and shear waves speed is approximately Vr = 0.92Vs. Given that the railroad track section surveyed here is limited to 140 km/h maximum speed, it is unlikely that the ground vibration boom conditions are ever reached, and hence the high amplitude arrivals seen here are caused by some other mechanism.

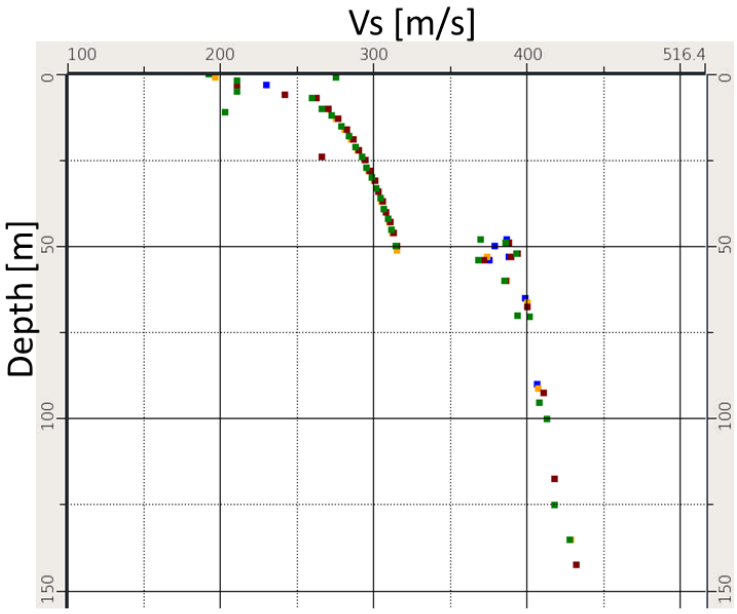

Figure 25. Shear wave speed Vs against depth from four shallow borehole measurements located nearest to the seismic array of the current study, published in [16].

Buildings & Proximity to Track

According to the RIVM survey report completed in 2014 [3] some 528 thousand people through the Netherlands live within a distance to the railroad track where train-induced vibrations can be felt and estimated to be below 3.2mm/s. We estimate the number of buildings surrounding the railroad tracks in Groningen (figure 26) that are located within roughly 50m of either side of the track. Some track sections in Groningen are electrified while others are not and are as a result serviced by diesel rolling stock. All track sections nevertheless are rated for train speeds of at least 80km/hr, generally consistent with the estimated speed of trains analysed in this report.

As demonstrated earlier (see figure 18), the amplitude of ground motion starts to decrease sharply at approximately 25 meters from the track. Assuming this distance across the region depicted in figure 26, we estimate around 179 occupied buildings that could be experiencing ≥1mm/s of ground vibrations daily, and in some instances perhaps hourly. The number of estimated buildings will vary depending on the details of how binning and counting is done; for example, the spatial positioning of bin coordinates and whether the centre or a corner of a building falls within the bin bounds. For the entire country of the Netherlands the number of structures within several distance bins is computed based on data from [17] and shown in figure 28.

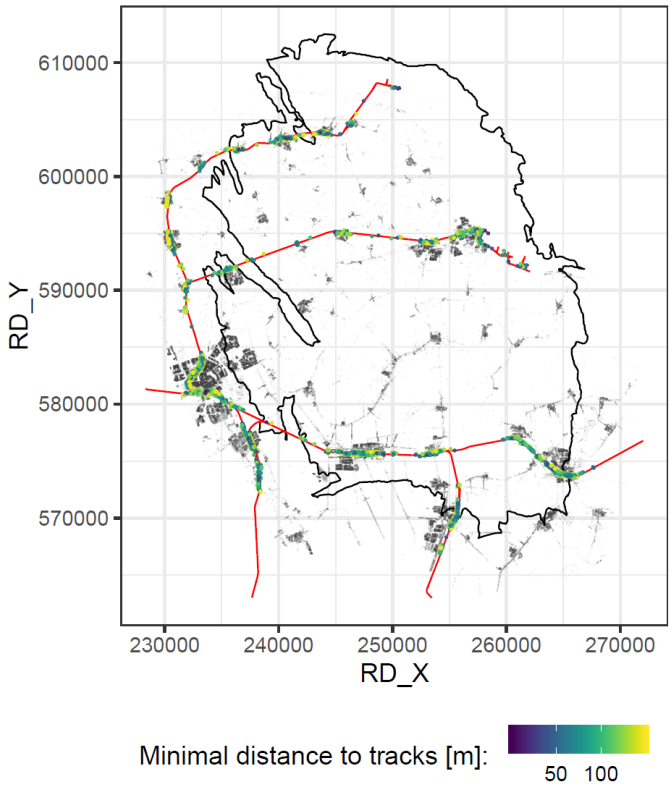

Figure 26. Map of train tracks (red lines) roughly covering the area of the Groningen gas field (black outline), highlighting 9516 structures situated within 150m of railways (roughly 75m from each side of the track).

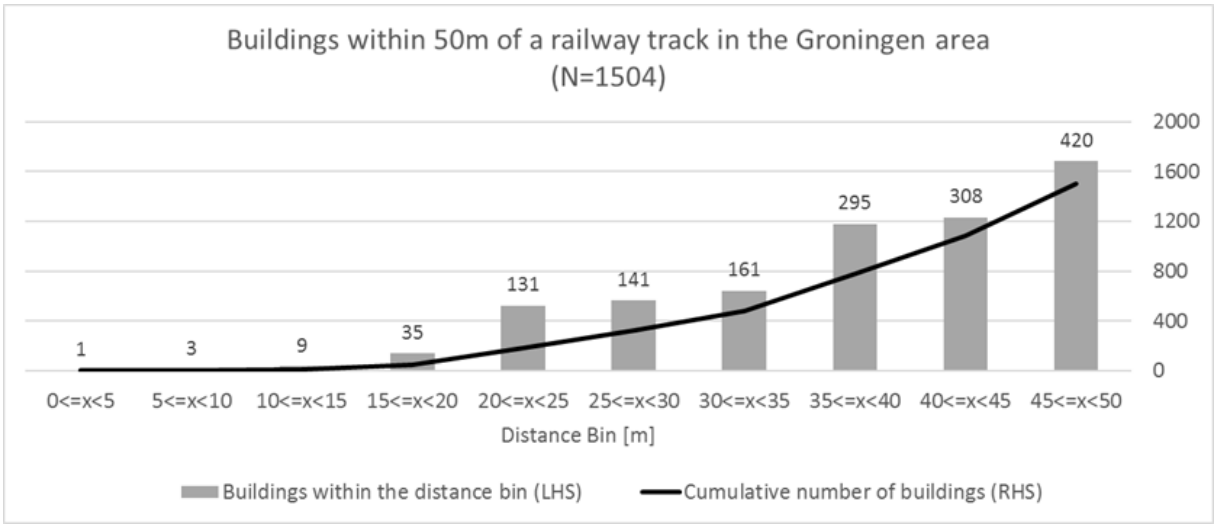

Figure 27. Estimate of occupied buildings with respect to distance to the railroad, for the area in figure 26.

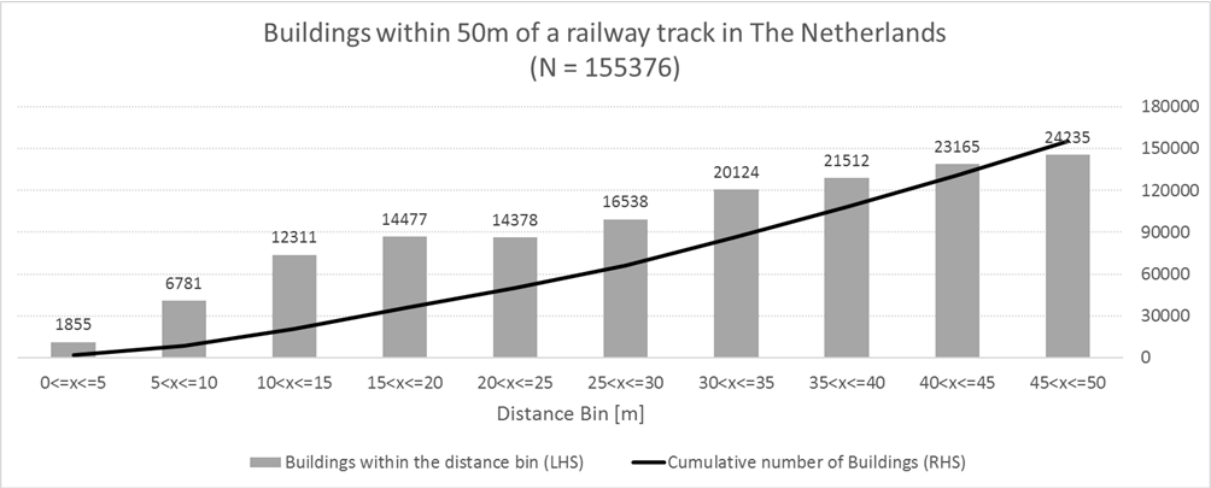

Figure 28. Estimate of all buildings, with respect to distance to the railroad, for the entire Netherlands.

Conclusions

1) Ground motions due to train passage were monitored for 56 days
    a. Monitoring network consisted of 77 3-component geophones
    b. Length of along-track array: ~100m at 15m distance to the track
    c. Length of array perpendicular to the track ~55m
2) Train-induced ground vibrations reached but never exceeded 3 mm/s SBR norm
    a. 3mm/s SBR vibration guideline was reached or exceeded 189 times (around three times a day)
    b. Ground motions exceeding 3 mm/s were not due to trains
    c. Highest velocity during survey was nearly 16 mm/s due to other urban source
3) 1mm/s ground velocity threshold was reached or exceeded 1913 times (more than once an hour)
    a. Although not all the exceedances were due to train passage, trains regularly cause vibrations between 1 and 3 mm/s (over 700 times in less than two months)
    b. Ground motion of 1mm/s is experienced as close as ~6.5km epicentral distance to the Zeerijp M3.4 earthquake
4) Train speeds were estimated in the range 70 – 90 km/h (lower than the track rating 140km/h)
5) Rayleigh wave velocities for the local soils are estimated at 200 m/s, in agreement with other studies
    a. Rayleigh wave ground boom condition is unlikely to be met
6) High variability in PGV observed station-to-station for a single train
7) High variability in amplitude response observed at a single station
8) To obtain a representative ground motion response, multiple metering stations are essential due to a high variability of recorder amplitudes

References

[1] Trillingen langs het spoor, ProRail, February 2017, accessible, via the link: https://www.prorail.nl/sites/default/files/brochuretrillingen_0.pdf

[2] European Macroseismic Scale 1998, EMS-98, Editor G. Grünthal, Chairman of the ESC Working Group "Macroseismic Scales" GeoForschungsZentrum Potsdam, Germany. [Online]. Available: http://media.gfz-potsdam.de/gfz/sec26/resources/documents/PDF/EMS-98_Original_englisch.pdf [Accessed August 18. 2018].

[3] RIVM.nl, "Wonen langs het spoor, Gezondheidseffecten van trillingen door treinen," RIVM Rapport 2014-0096, 23 Februari, 2015. [Online]. Available: https://www.rivm.nl. [Accessed June 10. 2018].

[4] A. Ditzel, "Train-induced ground vibrations: modelling and experiments," Ph.D. dissertation, Dept. Applied Math., Delft University of Technology, The Netherlands, 2003.

[6] D. Connolly, G. Kouroussis, P. K. Woodward, P. A. Costa, O. Verlinden, and M. C. Forde, "Field testing and analysis of high speed rail vibrations," Soil Dynamics and Earthquake Engineering, 67, 102-118, 2014. DOI: 10.1016/j.soildyn.2014.08.013

[5] V.V. Krylov, "Generation of ground vibrations by superfast trains," Applied Acoustics, 44, pp. 149-164, 1995.

[7] V.V. Krylov, "Ground vibration boom from high-speed trains," Journal of Low Frequency Noise, Vibration and Active Control, Vol 18, No 4, pp. 207-218, 1999.

[8] G. F. Miller, H. Pursey, Sir Edward Bullard, F. R. S., "On the partition pf energy between elastic waves in a semi-infinite solid." *Proc. R. Soc. Lond*. A 1955 233 55-69; 6 December 1955. DOI: 10.1098/rspa.1955.0245.

[9] "SBR Trillingsrichtlijn A: Schade aan bouwwerken: 2017." SBRCURnet, Delft November 2017. [Online]. Available: https://www.sbr.nl. [Accessed Aug. 10. 2018].

[10] H. Borsje, J. P. Pruiksma, M. Vasic, "Monitoring Network Building Vibrations – Analysis Earthquake 08-01-2018 (Zeerijp)," TNO 2018 R10743-B. [Online]. Available: https://nam-feitenencijfers.data-app.nl. [Accessed August 21 2018].

[11] M. Ntinalexis, J. J. Bommer, and B. Dost, "A Database of Ground-Motion Records from the Groningen Field Designated for the Development of the Groningen V3 GMPEs," A report prepared for NAM. Feb. 2016. [Online]. Available: http//NAM.nl. [Accessed Jul. 25. 2018].

[12] J. J. Bommer, P. J. Stafford, and M. Ntinalexis, "Empirical Ground-Motion Prediction Equations for Peak Ground Velocity from Small-Magnitude Earthquakes in the Groningen Field Using Multiple Definitions of the Horizontal Component of Motion," A report prepared for NAM. Feb. 2016. [Online]. Available: http//NAM.nl. [Accessed Jul. 29. 2018].

[13] J. Van Elk, T. Den Bezemer (editors), "Special Report on the Zeerijp Earthquake – 8th January 2018," A report prepared for NAM. Jan. 2018. [Online]. Available: http//NAM.nl. [Accessed Aug. 01. 2018].

[14] KNMI.nl, 2018. [Online]. Available: https://knmi.nl. [Accessed: July 22. 2018].

[15] Wikipedia.com, "Rail Transport in the Netherlands," 2018. [Online]. Available: https://en.wikipedia.org/wiki/Rail_transport_in_the_Netherlands. [Accessed: August 07. 2018].

[15] Dinoloket.nl, [Online]. Available: www.dinoloket.nl . [Accessed Aug. 01. 2018].

[16] P. P. Kruiver, A. Wiersma, F. H. Kloosterman, G. de Lange, M. Korff, J. Stafleu, F. S. Busschers, R. Harting, J. L. Gunnink, R. A. Green, J. Van Elk & D. Doornhof, "Characterisation of the Groningen subsurface for seismic hazard and risk modelling," *Netherlands Journal of Geosciences – Geologie en Mijnbouw*, 96 -5, s215-s233, 2017. DOI:10.1017/njg.2017.11.

[17] www.kadaster.com, [Online]. Available: www.kadaster.com . [Accessed 10/15/2018].